Parametric Studies of Transonic Flutter and Limit-Cycle Oscillation of an Aircraft Wing/Tip store

Srinivasan Janardhan, Ramana V. Grandhi,
Frank Eastep, Brian Sanders

Submitted in January 2003
to

JOURNAL OF AIRCRAFT

AIAA

A publication of the
American Institute of Aeronautics and Astronautics, Inc.
1801 Alexander Bell Drive, Suite 500
Reston, VA 20191–4344

Parametric Studies of Transonic Flutter and Limit-Cycle Oscillation of an Aircraft Wing/Tip Store

Srinivasan Janardhan[*], *Ramana V. Grandhi*[†]

Wright State University

Dayton, Ohio 45435

Frank Eastep[‡], *Brian Sanders*[§]

Air Force Research Laboratory

Wright-Patterson Air Force Base, Dayton, Ohio 45433

Abstract: This study investigates the effect of store parameters variation on store-induced flutter and limit-cycle oscillation phenomena of an aircraft wing in the transonic regime. The primary store parameters are its mass and the chordwise location of its center of gravity. The effect of including store aerodynamics on the wing/tip store configuration is also investigated. These studies are being conducted to understand the behavior of store-induced flutter and limit-cycle oscillation in the nonlinear region so as to limit the number of flutter flight tests to a few

[*] Graduate Research Assistant, Dept. of Mechanical & Materials Engineering, Wright State University, Dayton, Ohio 45435, Email: - sjanard@cs.wright.edu

[†] Distinguished Professor, Dept. of Mechanical & Materials Engineering, Wright State University, Dayton, Ohio 45435, Email: - rgrandhi@cs.wright.edu

[‡] NRC Senior Research Associate, Air force Research Laboratory, Wright-Patterson Air Force Base, Dayton, Ohio 45433, Email:- franklin.eastep@wpafb.af.mil

[§] Senior Aerospace Engineer, Air force Research Laboratory, Wright-Patterson Air Force Base, Dayton, Ohio 45433, Email:- Brian.Sanders@wpafb.af.mil

critical ones and enable in future store certification efforts. The tip store center of gravity (c.g.) has been varied and positioned at three different locations: 32.5%, 40%, and 50%, with respect to aerodynamic tip chord. Automated Structural Optimization System and Computational Aeroelasticity Program – Transonic Small Disturbance (CAP-TSD) have been used in the linear and nonlinear region to perform this research. Studies show that flutter speed increases as the store c.g. was moved forward towards the leading edge. This gives an indication that store c.g. must be placed as far forward as possible with respect to the elastic axis to delay the occurrence of flutter, while satisfying other design constraints. It was observed that the increase in tip store mass significantly reduced the flight operating speed range of the aircraft. The effect of inclusion of store aerodynamics for different wing/store configurations was found to be insignificant compared to their corresponding mass-only models in the transonic regime. LCO onset speed was found to be sensitive to store mass and varied significantly for different store mass configurations.

Keywords: store-induced flutter, LCO, CAP-TSD, ASTROS, aeroelasticity, transonic, sensitivity, store certification.

Introduction

Today's military aircraft can carry various configurations of external stores such as fuel tanks, missiles, bombs, and launchers. There are multiple positions available on the wing where attachment of stores is possible and one such position is at the wing tip. At the wing tip, again there are many combinations possible depending on the way store is attached. The presence and location of such external stores affect the structural, aerodynamic, and aeroelastic behavior of the wing. The mass or inertia parameters of the store also significantly affect the structural dynamic characteristics of the aircraft. Tip stores can change the aerodynamic and aeroelastic characteristics of a wing by the inertial, aerodynamic, and elastic coupling on the aircraft. The aeroelastic behavior of a tip store is very difficult to predict in the transonic region, as the governing equations in this region are highly nonlinear even under the assumption of small-disturbance, which makes the flow process very complex. These nonlinearities arise primarily due to the geometry of the wing (such as the thickness, camber, and angle of attack) and the presence of strong moving shocks on the wing surface. The presence of stores, especially tip stores, can cause significant dynamic aeroelastic effects such as flutter, and limit-cycle oscillation (LCO) in the transonic regime. They can lead to several problems in target-locking of an air to air missile attached at the wing tip and roll maneuverability of the entire aircraft. The occurrence of such unstable vibrations must be seriously considered and cleared off during the design of the wing structures. One of the main dynamic effects is LCO, which is generally encountered in external store configurations that are predicted to be flutter-sensitive. LCO, though not catastrophic as compared to classical flutter, can lead to fatigue, which reduces the efficiency and structural reliability of the wing. The store-induced LCO is characterized by the

antisymmetric motion of the wing and stores and a lateral motion of the fuselage and aircrew. It has been described as a self-sustaining oscillation with constant amplitude that occurs as a result of nonlinear coupling between the dynamic response of the structure and the unsteady aerodynamic forces. LCO has also been described in the past as oscillations, in which the amplitude of motion is limited, cyclic and oscillatory. Bunton and Denegri[1] have given a thorough description of LCO, its origin and differences when compared to classical flutter.

Earlier research was concentrated mainly on the prediction of flutter point and LCO of an aircraft wing/tip store configuration in the supersonic and subsonic regime using models of varying accuracy. The linear flutter analysis methods predicted the flutter boundary reasonably accurately in the subsonic regime due to the negligible effects of compressibility and aerodynamic nonlinearities in this region. Very little work was done in the transonic region, which most of the fighter aircraft pass through, while accelerating from subsonic region to supersonic region. There were no reliable computational tools that could predict the unsteady aeroelastic phenomena such as flutter and LCO. Also, no work was performed in studying the sensitivity of flutter and LCO by changing the store parameters in the transonic region, as that would have facilitated in better understanding of such phenomena. This paper concentrates primarily on the sensitivity of flutter and LCO behavior to store structural parameters such as store c.g. location and mass in the transonic region; the effect of including store aerodynamics on flutter for different wing/store configurations; and prediction, onset, occurrence and severity of store-induced flutter and LCO in the transonic region. This study was performed to assist in future store certification efforts, as large number of flutter flight tests are carried out to certify the stores attached to different aircraft. This results in a huge amount of cost, time, and work force being used for each flight test. This research facilitates in gaining a better understanding of

the behavior of flutter and LCO and developing a simulation-based design so as to reduce the number of flight tests to a few critical ones in the future store certification efforts.

The nonlinear aeroelastic analysis is performed using CAP-TSD, which has proven in the past to be accurate while performing unsteady aeroelastic analysis. CAP-TSD, a computational fluid dynamics (CFD) code, is based on the Transonic Small-Disturbance (TSD) theory. A wing structure was chosen on which flutter and LCO studies were conducted. Every effort was made to model the wing to possess real fighter aircraft wing characteristics. The finite element model is used to represent stiffness and mass properties of the wing and store. Vibration modes are used by CAP-TSD during the aeroelastic analysis to model the structure and are obtained from Automated Structural Optimization System (ASTROS[2]) modal analysis. Flutter analysis was carried out in both subsonic and transonic regimes using ASTROS and CAP-TSD to demonstrate the need for nonlinear aerodynamic analysis. However, LCO was found to occur mainly in the transonic region due to the addition of stores at various locations. Linear flutter analysis identified the frequency of oscillation and modal mechanism of LCO. However, due to the lack of effect of the nonlinearities, the linear flutter analysis failed to predict the onset or severity of LCO, which are extremely important during store certification efforts.

Previous Literature

In the past, Denegri[3] has investigated the response of an oscillatory wing during flutter flight tests of several external store configurations in the transonic region. He found that the response could be divided into various categories representing a broad range of aeroelastic responses encountered by a fighter aircraft with external stores. Chen *et al.*,[4] assumed that

nonlinear structural damping was a significant factor in the rise of a specific type of LCO, which occurred mainly in a low subsonic Mach number region. He conducted analysis on two aircraft configurations that differed only in the missile launcher positions; one underwing and the other on the wing tip. The results showed a "humped" damping curve with stability transitions, which correlated to the onset and subsequent stopping of the LCO, measured during flight-tests.

The influence of a tip store on transonic aeroelastic stability has also been examined by Guruswamy[5]. He conducted flutter analysis for rectangular and fighter type wings with tip stores using ATRAN3S code in the transonic region. It was shown that the tip store could make the wing aeroelastically unstable. However, no studies were conducted to investigate any variation of flutter or LCO behavior with store parameters. In the 1980s, Triplett[6] conducted linear flutter analysis on an F/A-18 wing carrying a tip store using the doublet-lattice method in the subsonic regime, but he did not analyze in the transonic region.

Turner[7] performed an analytical study on the effect of store aerodynamics using MSC/NASTRAN on a large number of wing/store configurations to develop general guidelines. However, it was possible only to generate specific guidelines for the inclusion of store aerodynamics for a particular aircraft. In another case, Striz and Jang[8] approximated the tip missile without fin geometry in the aerodynamic model and conducted their flutter analysis. Kim and Lee[9] performed aeroelastic analyses in the transonic and supersonic flow regions using a CFD technique (TSD3KR) for computing the unsteady aerodynamics in conjunction with MSC/NASTRAN for the flutter analysis of a wing with a tip store. They conducted a matched-point flutter analysis to obtain the flutter solutions in both the frequency and time domain. They showed that the effect of tip store could change the flutter stability of the wing structure significantly.

Jun *et al.*[10] have studied the influence of a wing tip missile on the multidisciplinary design optimization of a wing structure subjected to design constraints using ASTROS*[11]. Their studies indicated that the store aerodynamics must be included during the aft positioning of tip missile. All these studies were conducted for the subsonic and supersonic regions. The flutter behavior was found to be very sensitive to the tip missile position along the tip chord. Pitt and Fuglsang[12] have performed static and dynamic aeroelastic calculations on F-15 and F/A-18 wings using CAP-TSD. They have indicated the need for inclusion of nonlinear aerodynamics for both static and dynamic aeroelastic calculations in the transonic region, when compared with the corresponding linear analysis results. They effectively used CAP-TSD to demonstrate its capabilities to calculate aerodynamic effects, such as flutter, and aileron reversal speed, using TSD theory. However, no sensitivity studies with respect to store parameters on the variation in flutter and LCO were presented in their research. Kim and Strganac[13] analyzed LCO of an aircraft wing by considering structural, aerodynamic, and store-induced nonlinearities together. Recently, Beran *et al.*[14] has conducted CAP-TSD and ENS3DAE analyses on a Goland wing to determine the range of applicability of the various mathematical models in predicting the store-induced LCO.

Transonic Small-Disturbance Theory

CAP-TSD, developed by Batina[15], utilizes the TSD theory to solve unsteady aeroelastic problems in realistic aircraft configurations. The advantage of using TSD formulation is the relatively low computational cost, the simplicity of the gridding and geometry preprocessing, and the ability to treat complete aircraft configuration. The code uses a time-accurate approximate

factorization (AF) algorithm for an efficient solution of unsteady TSD equation. The AF algorithm consists of a time-linearization procedure coupled with an internal subiteration technique. For unsteady flow calculations, the solution procedure involves two steps. First, a time-linearization step is performed to determine an estimate of the potential field. Second, subiterations are performed to minimize the linearization and factorization errors. CAP-TSD is capable of treating combinations of lifting surfaces and bodies. In the TSD theory, the flow is assumed to be governed by a general frequency modified TSD potential equation written in conservation law form as

$$\frac{\partial f_0}{\partial t}+\frac{\partial f_1}{\partial x}+\frac{\partial f_2}{\partial y}+\frac{\partial f_3}{\partial z}=0 \tag{1}$$

where

$$f_0=-A\,\phi_t\ -B\,\phi_x \tag{2}$$

$$f_1=E\,\phi_x+F\,\phi^2{}_x+G\,\phi^2{}_y \tag{3}$$

$$f_2=\phi_y+H\,\phi_x\phi_y \tag{4}$$

$$f_3=\phi_z \tag{5}$$

The coefficients A, B and E are defined as

$$A=M_\infty^2,\ B=2M_\infty^2,\ E=1-M_\infty^2, \tag{6}$$

where M_∞ is the far-field Mach number and ϕ is the velocity potential.

F, G, and H depend on the assumptions used in deriving the TSD equation. For nonlinear analysis, the coefficients are

$$F=-\frac{1}{2}(\gamma+1)M_\infty^2,\qquad G=-\frac{1}{2}(\gamma-3)M_\infty^2\qquad H=-(\gamma-1)M_\infty^2, \tag{7}$$

and for linear analysis,

$$F = 0, \quad G = 0, \quad H = 0. \tag{8}$$

In the preceding equations, γ is the ratio of specific heat at constant pressure to specific heat at constant volume (1.4 for air). For steady flow calculations, after time-linearization, internal subiterations are not used because time accuracy is not necessary when marching towards steady-state. The solution of the TSD equation is the converged steady-state velocity potentials from which aerodynamic pressures are calculated. The aeroelastic computational procedure implemented within CAP-TSD includes the simultaneous integration of structural equations of motion and unsteady aerodynamic time-marching solution procedure.

Research Approach

The aeroelastic equations of motion for an elastic wing may be formulated in terms of generalized coordinates of modal motion $q(t)$, which is a solution to the following equation:

$$M\ddot{q} + C\dot{q} + Kq = Q(t) \tag{9}$$

where M is the generalized mass matrix, C is the generalized damping matrix, K is the generalized stiffness matrix, and $Q(t)$ is the vector of generalized aerodynamic forces that is discretized into Q_i by the splining technique. Q_i is the generalized aerodynamic force associated with q_i, which is computed by integrating the pressure distribution on the wing surface as

$$Q_i = \rho \frac{U^2 c_r^2}{2} \int_s h_i \frac{\Delta p}{\rho U^2/2} \frac{dS}{c_r^2} \tag{10}$$

$$\Delta C_p = \frac{\Delta p}{\rho U^2/2}$$

where ΔC_p is the coefficient of lifting pressure, ρ is the free stream air density, U is the free stream velocity, c_r is the reference chord length, S is the wing area, Δp is the difference in pressures between the lower and upper wing surfaces, and h_i is the i-th mode shape obtained by the infinite plate spline technique. h_i is obtained as

$$h_i = [G]\ x_i \tag{11}$$

where x_i is the structural mode shape and $[G]$ is the splining matrix, which interpolates the structural modes onto the aerodynamic grid.

Eq. 11 implies two steps:

a) Modal reduction of equations of motion.

b) Spline interpolation of forces and displacements from structural grid to aerodynamic grid and vice-versa.

The equation of motion (9) for the free vibration case can be rewritten as

$$\ddot{q} = -M^{-1}Kq - M^{-1}C\dot{q} \tag{12}$$

In the case of structural dynamic analysis, the above governing equation is solved (ignoring the aerodynamic forces term). This equation is solved using ASTROS to obtain the natural frequencies, mode shapes, generalized mass, and stiffness, which will be used by CAP-TSD to model the structure. The aeroelastic equations of motion in CAP-TSD are based on a right-hand orthogonal coordinate system with the x-direction defined as positive downstream and the z-direction positive upward.

Before the aeroelastic analysis is performed, the convergence of the CAP-TSD wing grid lines resolution is examined through steady-state aerodynamic calculations. Examining the wing

steady pressure helps to assess the basic character of the flow-field. The unsteady flow-field, and hence generalized aerodynamic forces, depend strongly on the steady-state flow, especially in the transonic speed range. Thus, the steady pressure distributions frequently can give mechanisms that control the aeroelastic phenomena.

Static aeroelastic analysis is performed using a value of dynamic pressure that is assumed to be near the velocity which produces flutter (neutral stability). For this, many simulation runs have to be executed. Static aeroelastic analysis yields a steady-state flow field, thus providing the starting flow-field for the dynamic aeroelastic analysis.

The dynamic aeroelastic analysis is initiated by restarting from the converged static aeroelastic solution. A small initial disturbance is given on the vertical velocity of the wing,

$$\dot{x}_0 = 1.0 \text{ in/sec} \tag{13}$$

From the above analysis, generalized displacements of each mode at each time step are obtained. Unsteady pressure distribution is also obtained from this analysis.

The coefficient of lift obtained from different instants of time is plotted. The damping ratio value is computed as

$$\delta_L = \frac{1}{n} \ln\left(\frac{A_n}{A_0}\right)$$

$$g = \frac{\delta_L}{\sqrt{4\pi^2 + \delta_L^{\,2}}} \tag{14}$$

where δ_L = log decrement

A_n = Amplitude of nth peak in C_L vs. time steps plot

A_0 = Amplitude of 1st peak in C_L vs. time steps plot

g = Damping ratio.

When the damping ratio value moves from a negative damping to a positive damping direction and crosses the zero damping, the flutter speed is obtained.

Wing Structure Model

In the initial phase, the wing structure used in Ref. 16 & 17 was considered. The present study required modifications in the above wing structure. In the previous studies, the semi-span for the structural model of the wing was 90 in., while the aerodynamic model span was 108 in. In order to attach the tip store aerodynamic model to the wing model, the structural semi-span was extended to the same length as the aerodynamic model. The structural model was extended by 20% of its original length so as to be completely superimposed by the aerodynamic model. The three spars were simply extended in their original directions for the required length.

The wing structure is a two-cell wing box. Figure 1 illustrates the finite element model of the wing structure. It has a root chord of 48 in. and a tip chord of 26.5 in. The semi-span is extended from 90 in. to 108 in. It is modeled using 120 finite elements, out of which 48 plate bending elements are used to represent the wing skins, 42 shear panels represent the spars, and ribs, and 30 rod elements represent the posts and are used to connect the upper and lower skin nodes. The material used is aluminum ($E=10.3 \times 10^6$ psi).

The wing root is built by fully constraining all the structural nodes at the root. No other constraints have been applied at other nodes and all have 6 degrees of freedom. The non-structural weight added at various structural nodes represents the weight of the structure outside (at the leading and trailing edges) and is attached to the wing and consists of other miscellaneous

weights, such as fuel, control system, etc. The non-structural weights have been distributed in such a way that each internal node carries 6 lbs., while each boundary node carries 9 lbs. The total non-structural weight was 378 lbs. There are no non-structural weights at the tip of the wing, as stores are attached at those points. The structural weight of the wing is 90.7 lbs. The rod cross-sectional area is set to 0.1 sq. in. The center of gravity is located at 46.14% of the root chord. The elastic axis is located at 44% of the root chord. The ratio of non-structural weight to structural weight is 4.16.

Wing Aerodynamic Model

An aerodynamic model, as shown in figure 2, was developed to provide unsteady aerodynamics for the ASTROS flutter analysis. The aerodynamic model for the wing planform is defined by 400 panels using doublet-lattice aerodynamics. There are 20 spanwise and 20 chordwise panels in the model. The spanwise and chordwise panels are equally spaced. The root chord and tip chord are 90 in. and 48 in., respectively. The wing semi-span is 108 in. The wing has an aspect ratio of 2.33. The aerodynamic parameters are calculated at aerodynamic grids, which do not generally coincide with the structural grid points. Splining technique was used to transfer the structural displacements and aerodynamic forces from one set of grids to the other.

In case of CAP-TSD, the wing was also modeled both in the physical and computational domain. The physical region boundary of the wing is defined in a similar manner as the ASTROS aerodynamic model. All the dimensions in CAP-TSD modeling were normalized using the reference chord length (in this case, aerodynamic root chord). The CAP-TSD computational grid for the wing chosen has 90 streamwise gridlines (with 50 gridlines per wing chord), 30 spanwise gridlines (with 20 gridlines on the wing), and 60 vertical grid lines.

Store Description

The store is attached to the wing at the tip. Figure 3 shows the structural model of the store connected to the wing at 50% of the aerodynamic tip chord. The store structural model is represented using BAR elements with seven grid points. The length of each element is uniformly distributed throughout the store. A model of six elements is developed to represent the store. The store is approximated without any fins and has a length of 79.5 in. The structural weight of the store is 154.1 lbs., and the non-structural weight added is 77 lbs. The non-structural weight represents the guidance and control system, etc. The store body is made of steel (modulus of elasticity: E= 30×10^6 psi; specific weight = 0.33 lb/ in^3). The area moments of inertia are $I_1=I_2=14.86$ in^4 and torsion constant, J= 29.72 in^4. The wing is joined to the store using BAR elements. It is assumed that the attachments are rigid. The stiffness of material used as attachments is very high compared to the stiffness of store. The attachments are configured in a V-shape. Each end of the connection element is attached to the top skin and bottom skin nodes of the wing tip.

Figure 4 shows the aerodynamic model of store attached to the wing at 50% aerodynamic tip chord. The model was generated using the ASTROS aerodynamic modeling scheme. The store was modeled as flat panels using doublet-lattice aerodynamics. The store model was generated using 25 panels and was divided in both chordwise and spanwise directions into 5 equal divisions each.

Results from ASTROS and Discussion

The natural frequencies and vibration mode shapes represent the dynamic characteristics of the wing model. Vibration analysis was performed on the clean wing and different wing/tip

store configurations using ASTROS. The mode shapes for a clean wing and a wing with tip store c.g. at 50% tip chord (mass-only) are shown in figures 5 & 6. There is a switching of modes from bending to fore-aft mode when the store is attached. The combination of a bending and torsional mode in the case of a clean wing has changed to a fore-aft mode due to store attachment. For a clean wing, the fourth mode is a fore-aft mode. This mode does not contribute anything to the dynamic characteristics and flutter behavior of the wing. The magnitude of frequency separation of the first and second modes for a clean wing is large compared to the separation between the third and the fourth modes. The vibration frequencies for a wing with the tip store c.g. at 50% tip chord (mass-only) have reduced by more than 50% when compared to the clean wing results. This is due to the inertia effect of the store attached to the wing. The mode shapes for 32.5% and 40% configuration are similar to the 50% configuration.

The flutter analysis was conducted for both subsonic and transonic Mach numbers in ASTROS. P-K method was used for the flutter speed calculations. A sea-level density ratio was maintained throughout the calculations. Velocity-Damping (V-g) diagram was used to locate the flutter point by computing the speed corresponding to zero damping value. In flutter analysis, the effect of store modeling on the wing was considered in two ways. In the first case, the store was considered a mass-only model. This means that the aerodynamics of the store was not included. The store contributed only inertia and structural characteristics. In the second case, aerodynamics of the store was also included along with the mass.

Figure 7 shows the V-g diagram for comparison of a clean wing and a wing/store configuration at 50% tip chord (both with and without store aerodynamics). The figure represents the effect of including the store aerodynamics on flutter speed. The analysis was conducted using ASTROS at a transonic Mach number of 0.9. However, one needs to remember that ASTROS

treats the transonic Mach numbers linearly. Therefore, the flutter speeds computed for transonic Mach numbers will have some inaccuracies due to the lack of nonlinearities. The first mode is the mode of instability showing a similar pattern of failure for both the mass-only model and the model with store aerodynamics. The flutter speed for the wing/tip store c.g. at 50% tip chord (mass-only) was found to be 545.025 knots, whereas the flutter speed for the same configuration with store aerodynamics included was 455.208 knots. There is a 16.48% decrease in flutter speed in the case of a wing/store configuration with store aerodynamics, when compared with the corresponding wing/store mass-only model. The severity of flutter can be determined from the fact that the wing/store model with store aerodynamics is rapidly becoming unstable, and the slope of instability curve is very steep compared to the wing/store mass-only model.

The flutter sensitivity to store c.g. location with respect to the wing aerodynamic tip chord was analyzed using different wing/store cases. The store was positioned in the same manner as the wing/tip store c.g. at 50% tip chord. In order to obtain the required configurations, the store was maintained at the same position, but the c.g. was moved to locate an exact position of 32.5%, 40%, and 50% with respect to the wing aerodynamic tip chord by redistributing the non-structural weight of the store.

The V-g plot showing flutter characteristics of the wing/store (mass-only) models at different store c.g. locations is shown in figure 8. The pattern of failure looks pretty much the same as the wing/store configuration with store aerodynamics, but the amplitude of damping is less for the mass-only model cases compared to the corresponding cases where the store aerodynamics is included. The results indicate that the tendency of the tip store to undergo flutter is less when it is attached closer to the leading edge when compared to other configurations.

Figure 9 shows a V-g diagram that represents the sensitivity of flutter with respect to different store c.g. locations (including store aero). As the store c.g. is moved aft of the elastic axis of the wing, the flutter velocity decreases rapidly. In all three wing/store configurations, the first mode is the mode of instability. The slope of instability becomes very steep when store c.g. is at 50% tip chord compared to other wing/store configurations and the clean wing. The flutter mode crosses the zero damping line locating the flutter point. However, the flutter mode crosses the zero damping line again after sometime, thus forming a "hump" mode. This gives an indication of the region in which LCO might occur, though linear flutter analysis fails to predict the onset or severity of LCO accurately due to lack of nonlinearities involved. As the store c.g. is moved aft of the elastic axis, the "hump" mode characteristics start to slowly disappear and the flutter characteristics start becoming dominant. This gives an indication that moving the store c.g. forward of the elastic axis will delay the occurrence of flutter.

Results from CAP-TSD and Discussion

In order to accurately predict the flutter speed and LCO onset speed in the transonic region by including the nonlinearities, an inviscid version of CAP-TSD was used. Aeroelastic analysis in CAP-TSD was carried out in generalized modal coordinates. The wing was modeled both in physical and computational regions. The aeroelastic analysis was performed for different values of velocity and dynamic pressure, assuming a constant sea-level density (unmatched flutter analysis). Structural damping was assumed to be zero for all cases. The angle of attack of the wing was taken as zero and a 90x30x60 grid was used to calculate the unsteady parameters for all the cases. Grid points were clustered along the edges and normal to the wing and store

geometry. The grid was generated externally by calculating grid-point distributions for all three of the coordinate directions. In CAP-TSD, the lifting surfaces are modeled as thin plates. The upper and lower surface data of each horizontal lifting surface is supplied to provide the thickness and camber information. The wing is modeled structurally using the first 6 modes while still retaining the characteristics of the basic flutter mechanism. These vibration modes were obtained from ASTROS modal analysis. The structural displacements were splined onto the aerodynamic grid of CAP-TSD.

The CAP-TSD dynamic aeroelastic analysis was performed in two stages. In the first stage, a static aeroelastic analysis was performed using nonlinear CAP-TSD aerodynamics. Static aeroelastic analysis results in a steady-state flow field to account for wing thickness, camber, and mean angle of attack, thus providing the starting flow field for the dynamic aeroelastic analysis. In the second stage, the dynamic aeroelastic analysis is initiated from the converged static solution by providing a small disturbance to each of the modal velocities to begin the structural integration. The disturbance in velocities for each mode was provided rather than displacements, as it helps in avoiding non-physical, strictly numerical transients and their possible instabilities. Figure 10 shows the unsteady pressure distribution for a clean wing at M=0.9 for a velocity V=669 knots on the computational grid. Transonic shock waves can be seen traveling from the root chord to the tip chord. The shocks drastically change the pressure distribution on the surface of the wing, thereby affecting the occurrence of flutter and LCO. This poses problems in correctly predicting the flutter speed for the given flow conditions. These shocks appear due to the nonlinear effects of mixed flow in the transonic region. The flutter speed was calculated by interpolating the various damping values to locate the speed

corresponding to zero damping. In the case of a clean wing, no LCO was found to occur in the transonic region.

Figure 11 shows the comparison of flutter speeds obtained using doublet-lattice aerodynamics and transonic small-disturbance theory in the linear subsonic region. The flutter speeds obtained using the two theories matched well at low Mach numbers. This was done to check for consistency in the linear region before moving onto the nonlinear region. Flutter boundaries were computed for clean wing and other wing/store configurations. For a clean wing, CAP-TSD predicted a flutter speed of 883 knots at Mach 0.7, a value 0.5% lower than that predicted by ASTROS. For the wing/store configuration at 50% tip chord, CAP-TSD predicted a flutter speed of 631 knots, a value 0.54% lower than that predicted by ASTROS. Similarly, CAP-TSD and ASTROS linear flutter analysis were conducted for the wing/store configurations at 3 store c.g. locations and compared. The flutter results were found to match well and as the Mach number increased, the difference in flutter velocities also increased due to the minor effects of nonlinearities in the high subsonic region.

Sensitivity in the behavior of flutter in the clean wing and the 3 wing/store (mass-only) configurations at different c.g. locations for different transonic Mach numbers is shown in Figure 12. The behavior was studied to examine the range of applicability of computed flutter speeds of an aircraft carrying tip store in the nonlinear region. It also indicates the sensitivity of flutter to different store c.g. locations in the transonic region. Here, the figure represents a flutter boundary for different Mach numbers that divides the region into a stable and unstable section. In this case, the inertia properties and aerodynamics of the wing alone were considered, where as only the inertia characteristics of the store was included. The wing and store structures were represented in the form of vibration modes. A "transonic dip" was observed at Mach 0.94 for the clean wing,

with a flutter velocity of 525 knots, while the "transonic dip" occurred at Mach 0.92 for the 3 wing/store configurations, thereby effectively reducing the flight envelope of the aircraft. It was observed that moving the store c.g. forward of the elastic axis, shifted the "transonic dip" to a higher flutter velocity at the same Mach number. The flutter boundary is very sensitive to the Mach number for all the configurations near the "transonic dip" region. The occurrence of "transonic dip" is due to the presence of shock waves that increase in strength and move as the Mach number increases. The dip is characterized by a sudden drop in flutter speed before rising again at high transonic Mach numbers.

Figure 13 represents the sensitivity of flutter speed to store inertia parameter, namely the tip store mass. In this analysis, only the wing with tip store c.g. at 50% configuration was chosen, since this represents the extreme case of flutter as shown in the previous case. In the first case, the initial non-structural mass is used and then the store non-structural mass (NSM) was assigned twice the initial store NSM, and in the third case, it was made three times. It was earlier found that a "transonic dip" occurs at M=0.92 when the initial store mass is attached, but no such behavior was observed when the store mass was increased. The disappearance of transonic dip for heavier store configurations could be related to the coupled aeroelastic nonlinearities involved in the transonic flow process. In fact, as the non-structural store mass was doubled or tripled, the flutter speed kept decreasing with the Mach number even beyond M=0.92. This indicates that increasing the store mass can lead to a decrease in the range of flight speeds in which a fighter aircraft can operate. As the store mass is increased, the percentage difference in flutter velocity between any two successive configurations is decreasing. There is a steep drop in flutter velocity after M=0.9.

The impact of including the store aerodynamics while modeling the store in the transonic region has also been studied. This study was carried out to facilitate in deciding whether store aerodynamics need to be included while performing multidisciplinary design optimization of the wing structure to delay the occurrence of store-induced flutter and LCO in the transonic region. The optimization algorithms are highly iterative in nature and computationally intensive; therefore, including the store aerodynamic model could make the whole procedure even more time-consuming and difficult. In order to understand the impact of including the store aerodynamics in the nonlinear region, flutter speeds of different store mass configurations are represented in figure 14. The flutter speeds due to store aerodynamics for the 3 store mass configurations did not vary significantly when compared to their corresponding mass-only cases. The overall percentage difference was in the range of approximately 0 – 7%, based on all of the cases in the transonic regime. This range of difference in flutter speeds, matches well with the results reported by Turner[7]. For some cases, the flutter speed computed for store aerodynamics matched almost exactly with their corresponding mass-only cases. The flutter speed for wing/tip store at 50% mass-only configuration was 450 knots, while for the corresponding store aerodynamics case was 425.67 knots at a Mach 0.9. The percentage difference was approximately 5.4%. For the same case, the linear theory failed to correctly predict the flutter speed in the transonic regime. Actually, the impact of including store aerodynamics on the flutter speed depends on the problem and in this case, the inclusion of store aerodynamics, while modeling the store, did not have any significant effect when compared to the corresponding mass-only model. Another interesting thing observed is that in the case of the wing/store configuration at 50% aerodynamic tip chord, the flutter speed, when the store aerodynamics is

included, is more than the corresponding mass-only configuration for higher transonic Mach numbers (Mach 0.94, 0.96), compared to lower transonic Mach numbers (Mach 0.8, 0.9, 0.92).

Figure 15 shows the sensitivity of LCO onset speed to store mass computed for a range of transonic Mach numbers for the 3 wing/tip store configurations using CAP-TSD. LCO was observed to occur mainly in a restricted Mach number range. For all of the wing/store configurations, LCO occurred only after Mach 0.9. No LCO was observed in the linear region and the initial transonic region. This is because of the fact that LCO is a highly nonlinear phenomenon, due to which the linear aerodynamic theories are unable to capture its occurrence. The LCO onset speed was computed for each wing/store configuration in the high transonic Mach number range (0.9 – 0.96). The LCO onset speed was found to decrease rapidly as the store mass was increased. For a given Mach number 0.94, the LCO onset speed reduced by approximately 13%, as the store non-structural mass was first doubled and then tripled. The slope of the LCO curve for each configuration was approximately the same. Severity of LCO over a transonic Mach number range can be observed in the steep slope of the curve for each configuration, indicating that the addition of store mass for a given configuration might create a greater tendency to undergo LCO in the transonic regime. Figure 16 shows LCO occurring at V=380 knots for the wing with store c.g. at 50% tip chord (mass-only). The amplitude of the LCO was found to be quite large, representative of the characteristics of the nonlinear phenomena in the transonic region.

Summary/Conclusions

This study was intended to analyze the effect of varying the store parameters on different wing/store configurations in the transonic region and provide more information to enable in

future store certification efforts. The store structural parameters investigated are location of store c.g. with respect to the aerodynamic tip chord and store mass. The effect of including store aerodynamics was also investigated for different wing/store configurations in the transonic regime.

Linear aeroelastic analysis results using ASTROS for clean wing and different wing/store c.g. configurations matched well with the CAP-TSD linear analysis results for their corresponding configurations. This was done to check for consistency in the linear region before entering the nonlinear (transonic) region.

Comparisons of flutter results for the clean wing and wing/store configurations for different store c.g. locations using ASTROS were presented. Flutter results were presented for clean wing and a particular (store c.g. at 50% tip chord) wing/store configuration (mass-only model) using CAP-TSD. In both cases, it was found that moving the store c.g. forward relative to the elastic axis has a stabilizing effect by increasing the flutter speed. Therefore, the store should be attached as far forward as possible, simultaneously satisfying other design constraints so as to delay the occurrence of flutter.

Addition of store aerodynamics decreased the flutter speed of the wing/store configuration by 16.48% as compared to the store mass-only model, when doublet-lattice aerodynamic theory was used for flutter prediction. However, the TSD theory did not indicate much difference in flutter results between the mass-only model and the store aerodynamics model. Overall, the difference in flutter speeds for the two types of configurations was found to be in the range of 0-7% in the nonlinear region that matched well with the results reported in a previous paper.

"Transonic dip" was found to occur at an earlier Mach number in the wing/store configurations compared to the clean wing. This could effectively reduce the flight envelope of the aircraft and thereby inhibit the accomplishments of the mission critical tasks. Sensitivity of flutter speed to the store mass was also analyzed, and it was found that increasing the store mass reduced the flutter speed significantly. "Transonic dip" was found to occur for an initial store mass for the given configuration, but as the store mass was increased, the behavior disappeared. For higher Mach numbers and store mass values, the flutter speed was found to decrease rapidly. No occurrence of LCO was found in the clean wing configuration throughout the transonic Mach number range. Store-induced LCO onset speed was found to be very sensitive to the store mass in the transonic regime. The LCO onset speed decreased rapidly in the highly nonlinear region with increase in store mass. This LCO behavior with respect to the Mach numbers could pose several problems in flying an aircraft in the operating speed range.

Acknowledgements

This research work has been sponsored by the Air Force Office of Scientific Research (AFOSR) under the Grant F49620-01-1-0179. The authors acknowledge the support of Narendra S. Khot and Phil Beran of Wright-Patterson Air Force Base, Ohio, for their valuable suggestions and John Edwards and David M. Schuster of NASA Langley Research Center, Hampton, Virginia, for providing the CAP-TSD code.

References

1. Bunton R.W. and Denegri Jr. C.M., "Limit Cycle Oscillation characteristics of fighter aircraft", *AIAA Journal of Aircraft*, Vol. 37, No. 5, October 2000, pp. 916-918.

2. Johnson E., and Venkayya V.B. "Automated Structural Optimization System (ASTROS)", Volume-I Theoretical Manual, U.S. Air Force Wright Aeronautical Labs. TR-88-3028 (1988).

3. Denegri Jr., C.M. "Limit Cycle Oscillations flight test results of a fighter with external stores.", *Proceedings of 41st AIAA/ASME/ASCE/AHS/ASC Structures, Structural Dynamics and Material Conference and Exhibit*, Atlanta, GA, 3-6 April, 2000.

4. Chen, P.C., Sarhaddi, D. and Liu, D.D. "Limit-cycle oscillation studies of a fighter with external stores", *Proceedings of 39th AIAA/ASME/ASCE/AHS/ASC Structures, Structural Dynamics and Material Conference and Exhibit*, AIAA-98-1727, April 1998.

5. Guruswamy, G.P., Goorjian, P.M. and Tu, E.L. "Transonic Aeroelasticity of wings with Tip stores" *AIAA paper* 86-1007, 672-682.

6. Triplett, W.E. "Wind tunnel correlation study of aerodynamic modeling for F/A-18 wing-store tip-missile flutter", *AIAA Journal of Aircraft*, Vol. 21, No. 8, 1984, pp. 329-334.

7. Turner, C. "Effect of store aerodynamics on wing/store flutter", *AIAA Journal of Aircraft*, Vo. 19, No.7, 1982, pp. 574-580.

8. Striz, A.G. and Jang, S.K. "Optimization of wing tip store modeling", *AIAA Journal of Aircraft*, Vol. 24, No. 8, 1987, pp. 516-517.

9. Kim, D. and Lee, I. "Transonic and supersonic flutter characteristics of a wing-box model with tip stores", *Proceedings of 42nd AIAA/ASME/ASCE/AHS/ASC Structures, Structural Dynamics, and Material Conference and Exhibit*, Seattle, WA, 16-19 April, 2001.

10. Jun, S., Tischler, V.A. and Venkayya, V.B. "Multidisciplinary design optimization of a built-up wing structure with tip missile", *Proceedings of 43rd AIAA/ASME/ASCE/AHS/ASC Structures, Structural Dynamics and Materials Conference and Exhibit*, April 22-25, 2002, Denver, Colorado, AIAA-2002-1421.

11. Chen P., Sarhaddi D., and Liu D. "Development of the Aerodynamic/Aeroservoelastic Modules in ASTROS" Volume 2: *ZAERO Programmer's Manual*, Air force Research Laboratory, AFRL-VA-WP-TR-1999-3050 (1999).

12. Pitt, D. M. and Fuglsang, D. F. "Aeroelastic Calculations for fighter aircraft using the transonic small disturbance equation", *Paper no. 16 in Transonic Unsteady Aerodynamics and Aeroelasticity*, AGARD CP 507, March 1992.

13. Kim, K., and Strganac, T.W. "Aeroelastic studies of a cantilever wing with structural and aerodynamic nonlinearities.", *Proceedings of 43rd AIAA/ASME/ASCE/AHS/ASC Structures, Structural Dynamics and Materials Conference and Exhibit*, April 22-25, 2002, Denver, Colorado, AIAA-2002-1412.

14. Beran, P.S., Khot, N.S., Eastep, F.E., Snyder, R.D., Zweber, J.V., Huttsell, L.J., and Scott, J. N. "The Dependence of Store-Induced Limit-Cycle Oscillation Predictions on Modelling Fidelity," *Proceedings of the RTO Applied Vehicle Technology Panel Symposium on "Reduction of Military Vehicle Acquisition Time and Cost through Advanced Modeling and Virtual Product Simulation,"* Paris, France, 22-25 April, 2002, paper #44.

15. Batina, J.T., Seidal, D.A., Bland, S.R. and Bennett, R.M. "Unsteady Transonic Flow Calculations for Realistic Aircraft Configurations, AIAA Paper No. 87-0850, *Proceedings of 28th AIAA/ASME/ASCE/AHS Structures, Structural Dynamics and Materials Conference and Exhibit*, Monterey, CA, April 2-4, 1990.

16. Wilkinson K., Lerner E. and Taylor R.F., "Practical design of minimum-weight aircraft structures for strength and flutter requirements", *AIAA Journal of Aircraft*, Vol. 13, No. 18, 1976, pp. 614-624.

17. Hemmig, F.G., Venkayya, V.B. and Eastep, F.E. "Flutter speed degradation of damaged, optimized flight vehicles.", *AIAA Journal of Aircraft*, Vol. 17, No. 12, 1980, pp. 833-834.

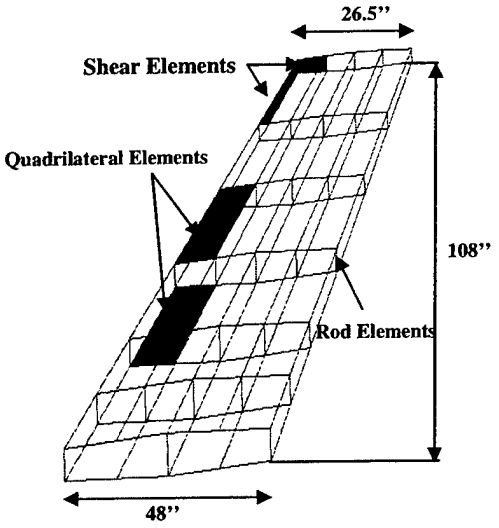

Figure 1: Wing Structure finite element model

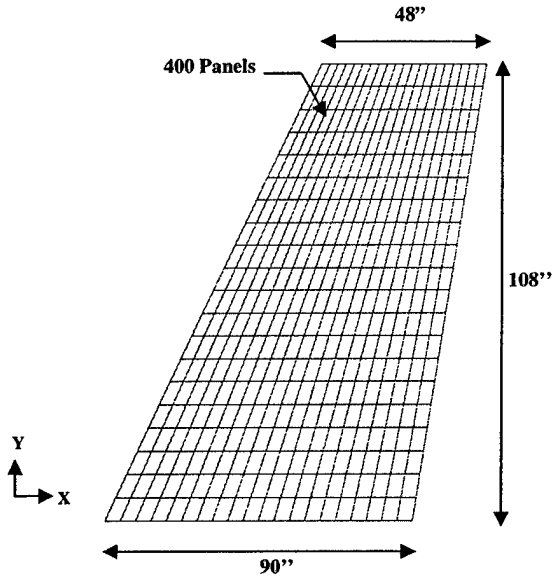

Figure 2: Aerodynamic model of wing

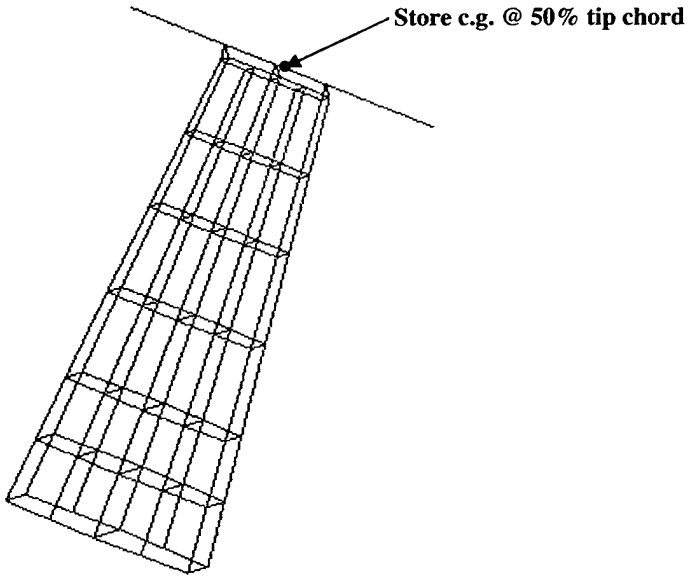

Figure 3: Finite element model of wing with tip store c.g. at 50% tip chord

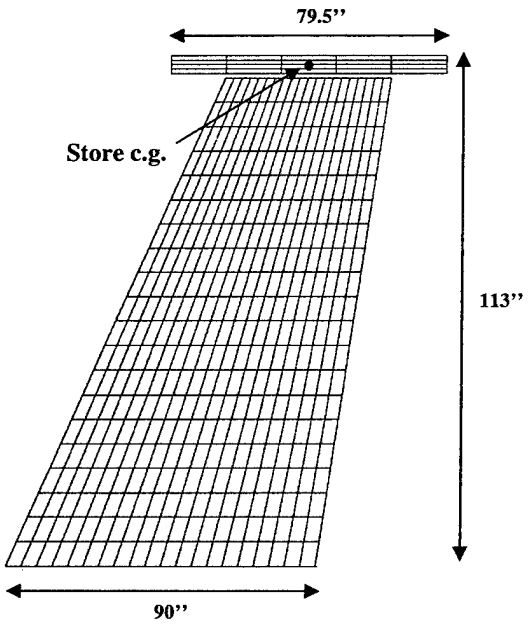

Figure 4: Aerodynamic model of wing with tip store c.g. at 50% tip chord

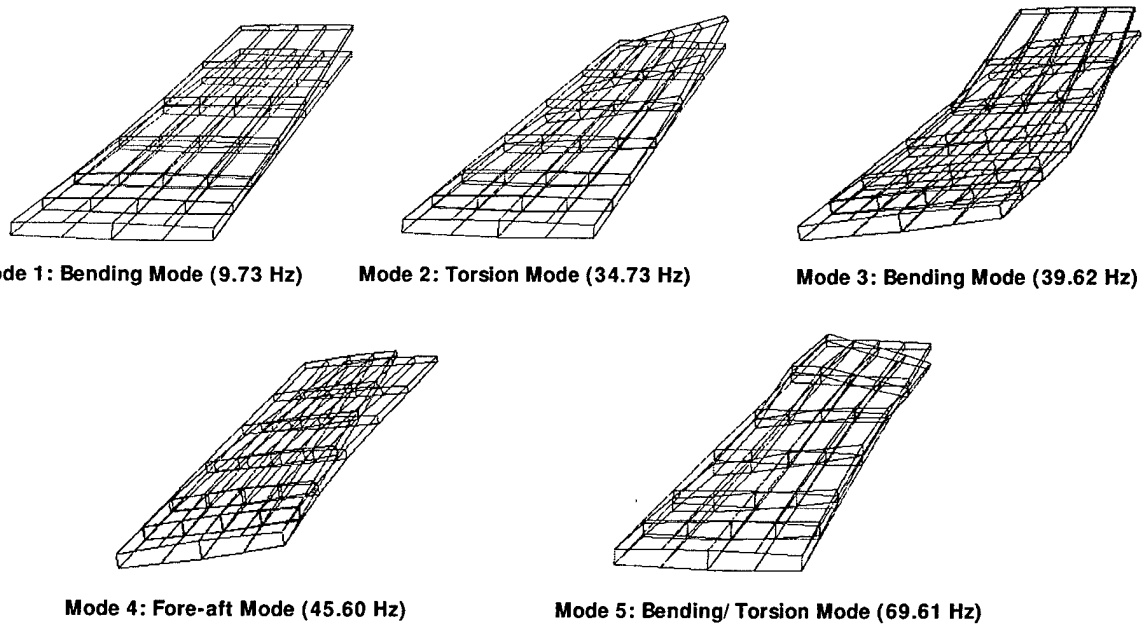

Mode 1: Bending Mode (9.73 Hz) Mode 2: Torsion Mode (34.73 Hz) Mode 3: Bending Mode (39.62 Hz)

Mode 4: Fore-aft Mode (45.60 Hz) Mode 5: Bending/ Torsion Mode (69.61 Hz)

Figure 5: Mode shapes of clean wing

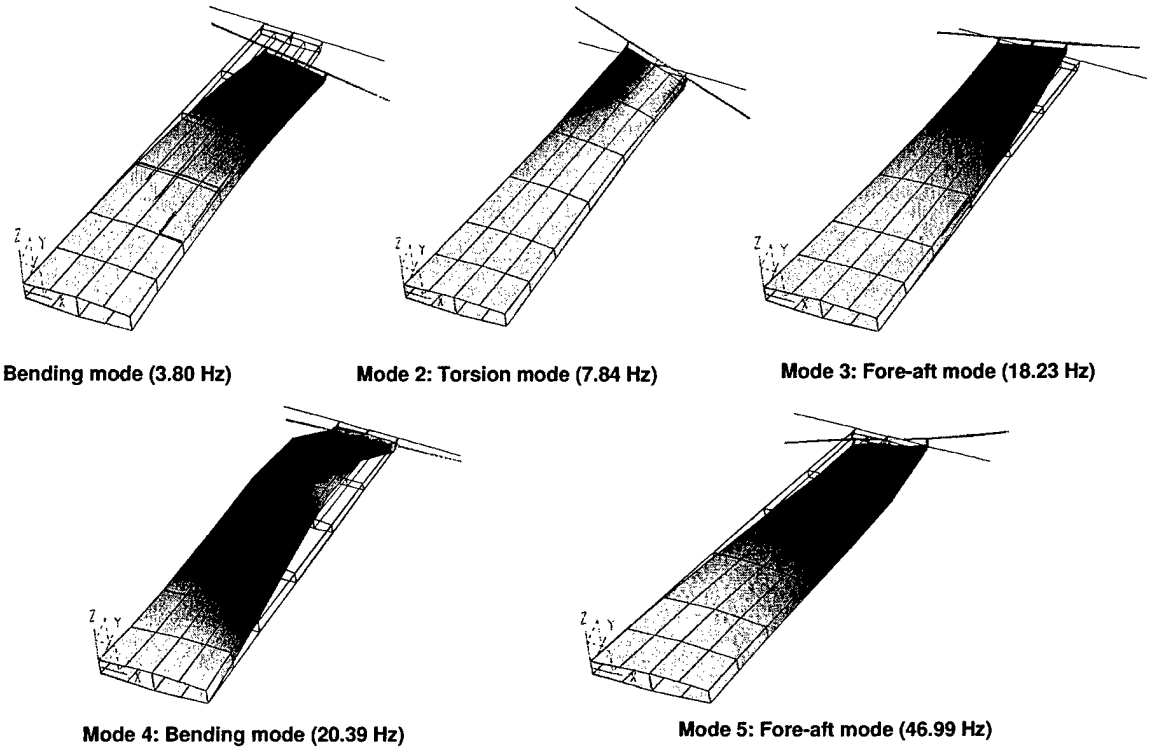

Mode 1: Bending mode (3.80 Hz) Mode 2: Torsion mode (7.84 Hz) Mode 3: Fore-aft mode (18.23 Hz)

Mode 4: Bending mode (20.39 Hz) Mode 5: Fore-aft mode (46.99 Hz)

Figure 6: Mode shapes of wing with store c.g. at 50% tip chord

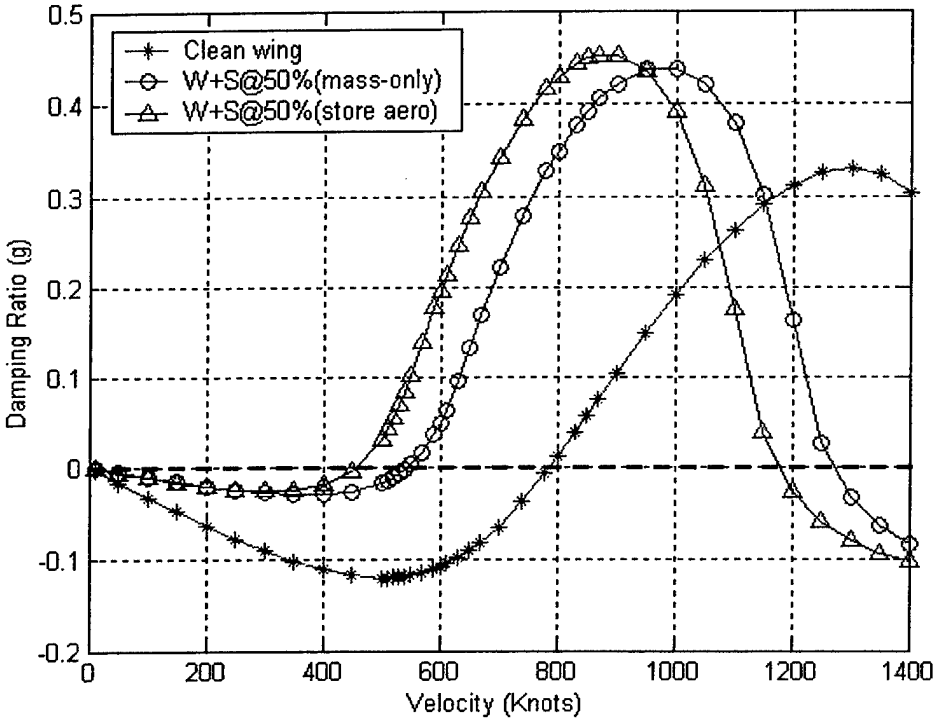

Figure 7: V-g plot showing the effect of including store aerodynamics on flutter (ASTROS)

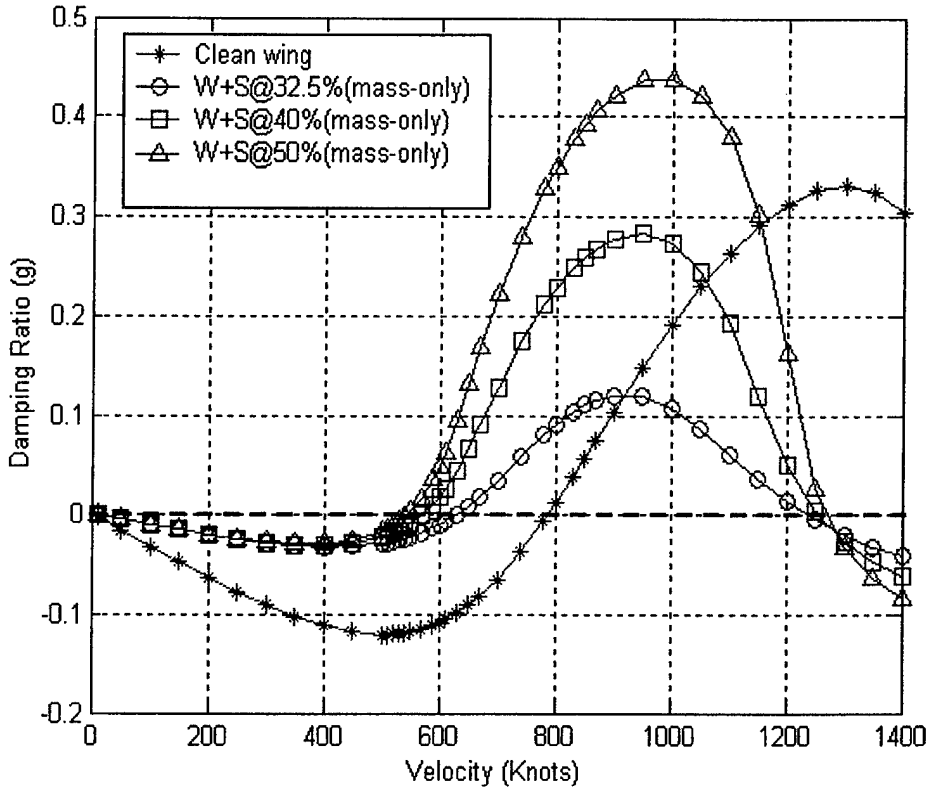

Figure 8: V-g plot for sensitivity of flutter to store c.g. location using different wing/store (mass-only) models

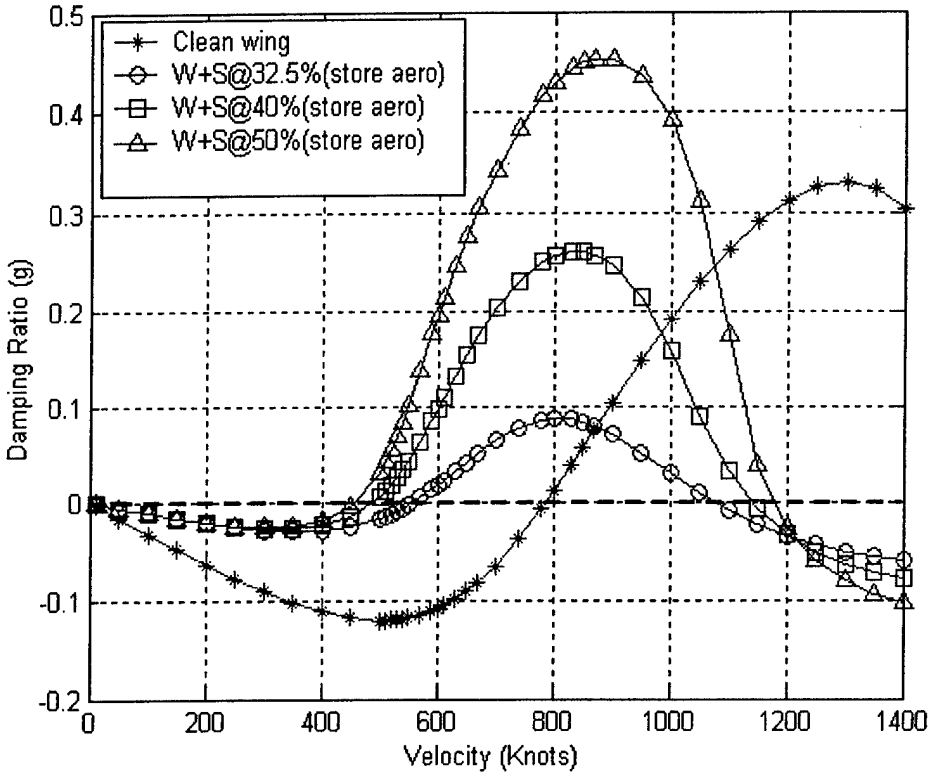

Figure 9: V-g plot for sensitivity of flutter to store c.g. location using different wing/store (store aero) models

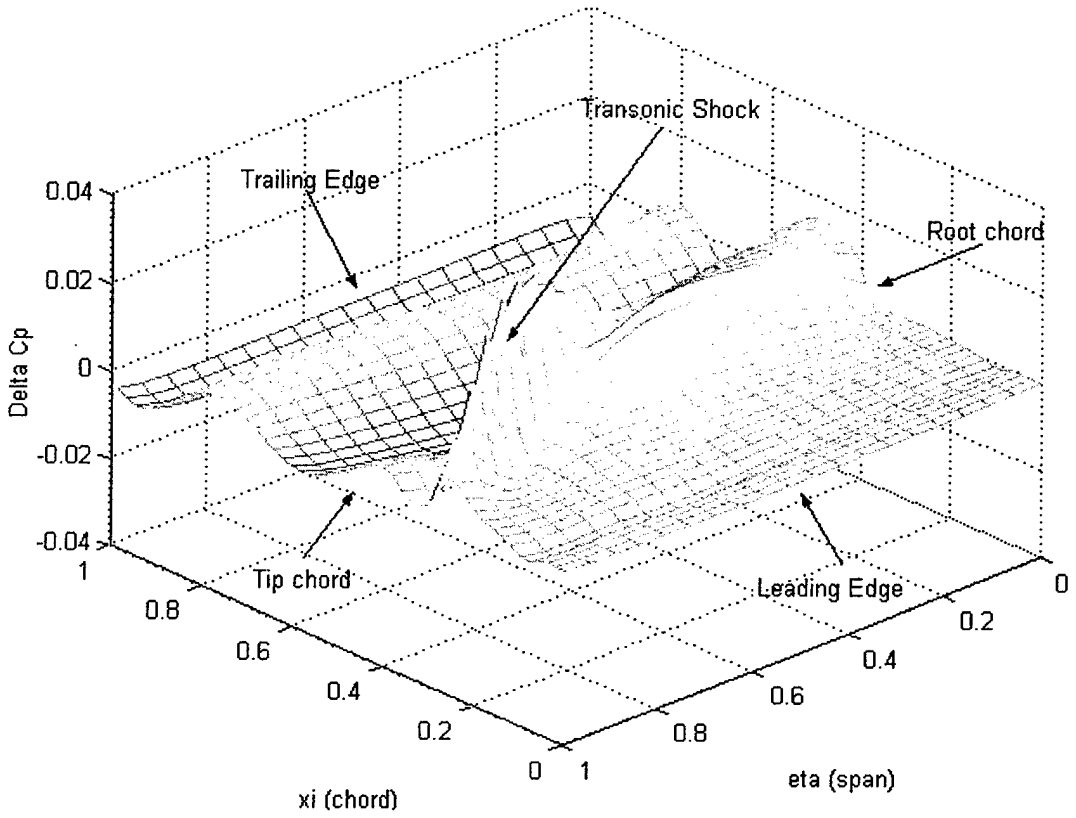

Figure 10: Unsteady Pressure Distribution for a clean wing at V=669 Knots, M=0.9

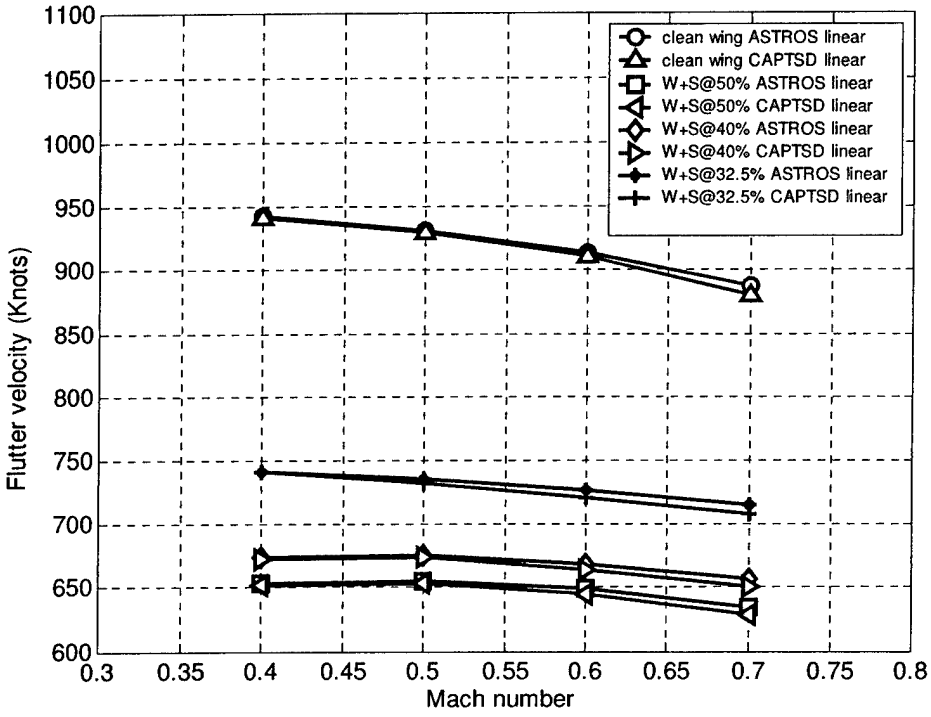

Figure 11: Comparison of linear flutter analysis for different store c.g. configurations

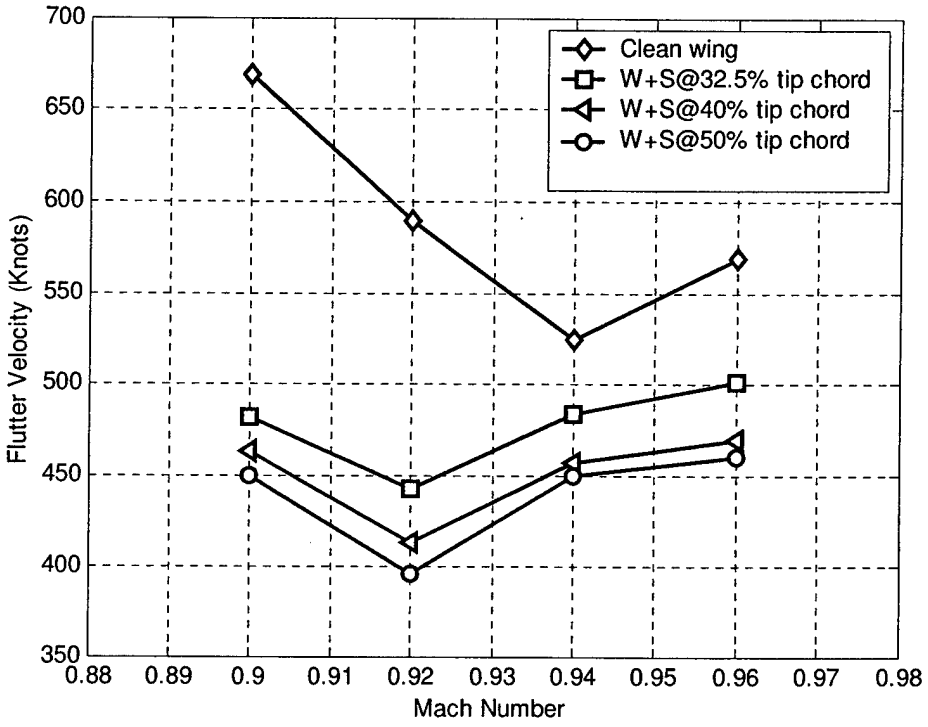

Figure 12: Sensitivity of flutter velocity to store c.g. location for transonic Mach numbers (mass-only models)

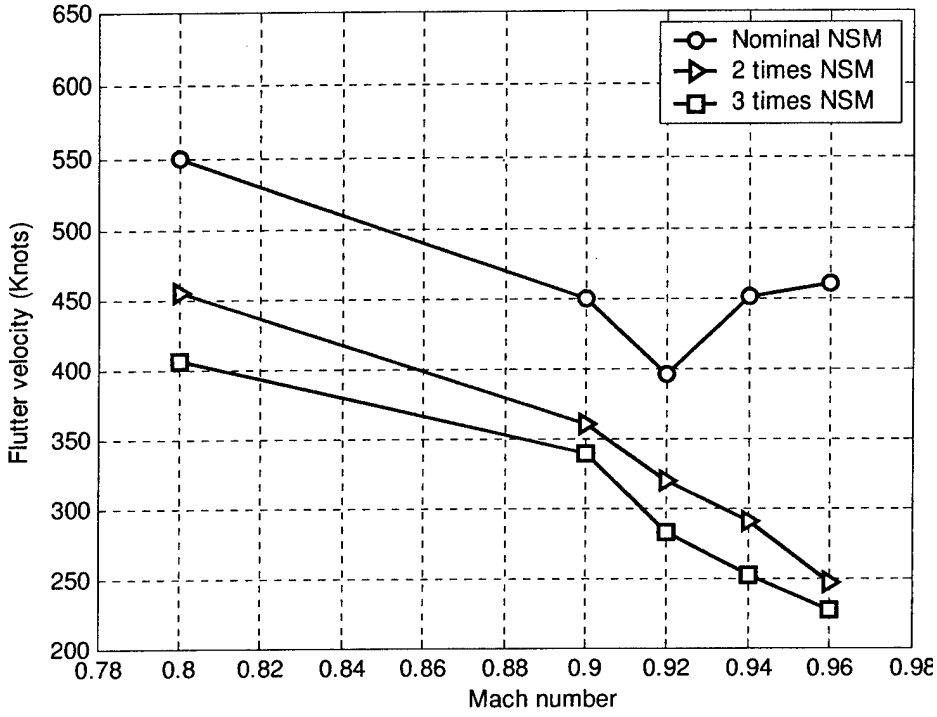

Figure 13: Sensitivity of flutter velocity to store mass for transonic Mach numbers

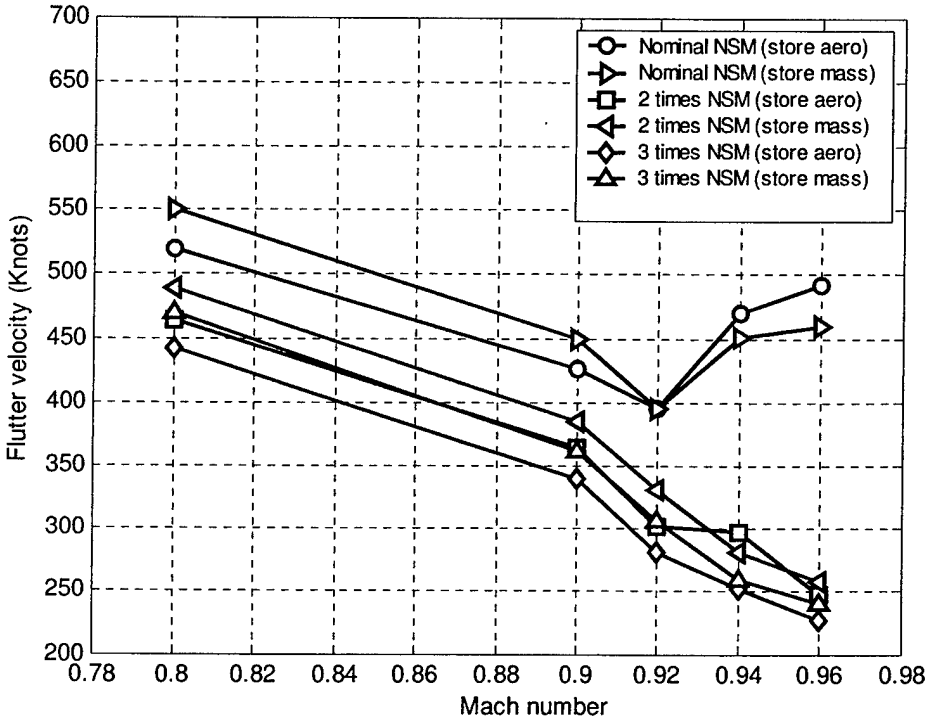

Figure 14: Effect of inclusion of store aerodynamics in the transonic regime

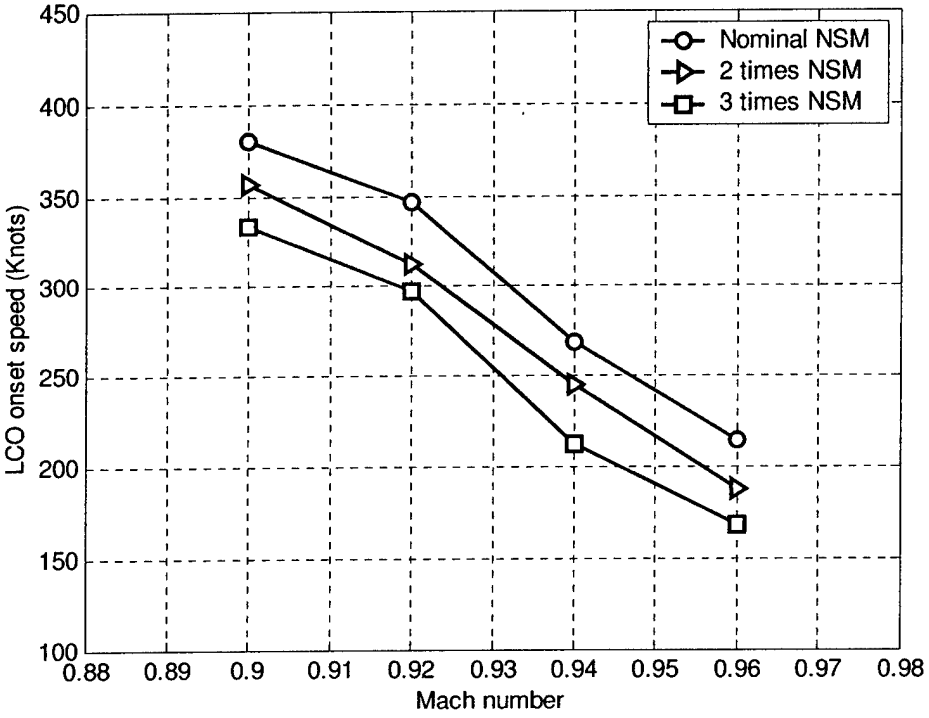

Figure 15: Sensitivity of LCO onset speed to store mass for transonic Mach numbers

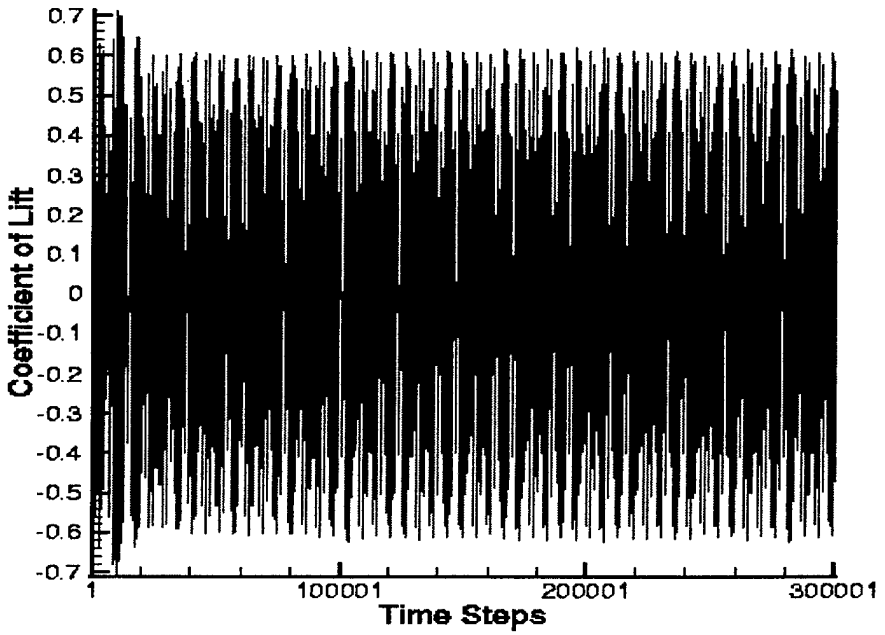

Figure 16: Wing with tip store c.g. @50% (mass-only) showing LCO at 380 knots at M=0.9.